ACS Energy LETTERS

http://pubs.acs.org/journal/aelccp

LETTER

Revealing the Active Phase of Copper during the Electroreduction of CO_2 in Aqueous Electrolyte by Correlating *In Situ* X-ray Spectroscopy and *In Situ* Electron Microscopy

Juan-Jesus Velasco-Velez,* Rik V. Mom, Luis-Ernesto Sandoval-Diaz, Lorenz J. Falling, Cheng-Hao Chuang, Dunfeng Gao, Travis E. Jones, Qingjun Zhu, Rosa Arrigo, Beatriz Roldan Cuenya, Axel Knop-Gericke, Thomas Lunkenbein, and Robert Schlögl

Cite This: *ACS Energy Lett.* 2020, 5, 2106−2111

Read Online

ACCESS | Metrics & More | Article Recommendations | Supporting Information

ABSTRACT: The variation in the morphology and electronic structure of copper during the electroreduction of CO_2 into valuable hydrocarbons and alcohols was revealed by combining *in situ* surface- and bulk-sensitive X-ray spectroscopies with electrochemical scanning electron microscopy. These experiments proved that the electrified interface surface and near-surface are dominated by reduced copper. The selectivity to the formation of the key C−C bond is enhanced at higher cathodic potentials as a consequence of increased copper metallicity. In addition, the reduction of the copper oxide electrode and oxygen loss in the lattice reconstructs the electrode to yield a rougher surface with more uncoordinated sites, which controls the dissociation barrier of water and CO_2. Thus, according to these results, copper oxide species can only be stabilized kinetically under CO_2 reduction reaction conditions.

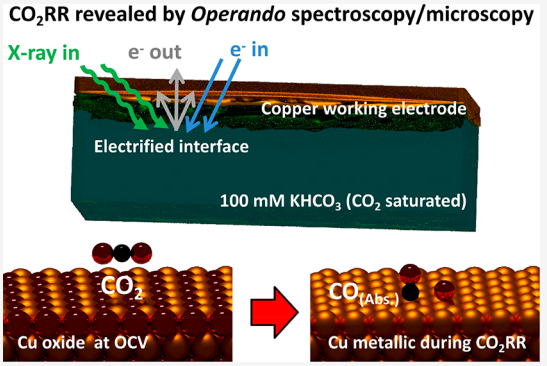

Closing the carbon loop toward a clean energy economy requires the reduction of CO_2 emissions using substitute fuels for powering engines. Other solutions entail the sequestration of CO_2 by pulling it out of the atmosphere and burying it in geologic reservoirs. Combining the two previous concepts yields another approach, wherein CO_2 is pulled out of the air and transformed into valuable chemical feedstocks via electrochemistry,[1−5] yielding a negative carbon cycle if this process is powered with renewable sources of energy. Among the different chemical elements, copper can uniquely perform the electrocatalytic reduction of CO_2 into valuable hydrocarbons and alcohols.[6−9] Unfortunately, the cathodic CO_2 reduction reaction (CO_2RR) suffers from low current density, high overpotential,[10,11] low selectivity, and electrode deactivation over time,[12] hindering its industrial application.[13] Consequently, the understanding of Cu activation in the electrocatalytic reduction of CO_2 is a crucial factor to develop highly active, selective, and stable electrocatalysts[14] because of its unique property to produce the C−C bond. Surface-sensitive spectroscopies during electrochemical reaction can shed light on this issue, but it is technically challenging to realize such measurements.[15] Thus, revealing the electronic structure of copper during the electrochemical reduction of CO_2 requires the use of element-specific techniques and the combination of surface- and bulk-sensitive detection schemes in order to identify the catalyst's active centers.[16−18] Furthermore, these changes in the electronic structure of the catalyst are accompanied by modifications in the electrode morphology requiring microscopy characterization for the complete process understanding.

Element-specific X-ray spectroscopy is used for the investigation of catalysts during reaction conditions, though it is technically challenging in the soft X-ray regime. A bulk-sensitive version has been realized by thin Si_3N_4 membranes that separate the liquid phase from vacuum allowing the collection of photons in a total fluorescence yield mode (TFY).[19,20] Another approach is to record the intensity decay of the incoming X-ray

Received: April 13, 2020
Accepted: May 27, 2020
Published: May 27, 2020

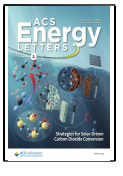

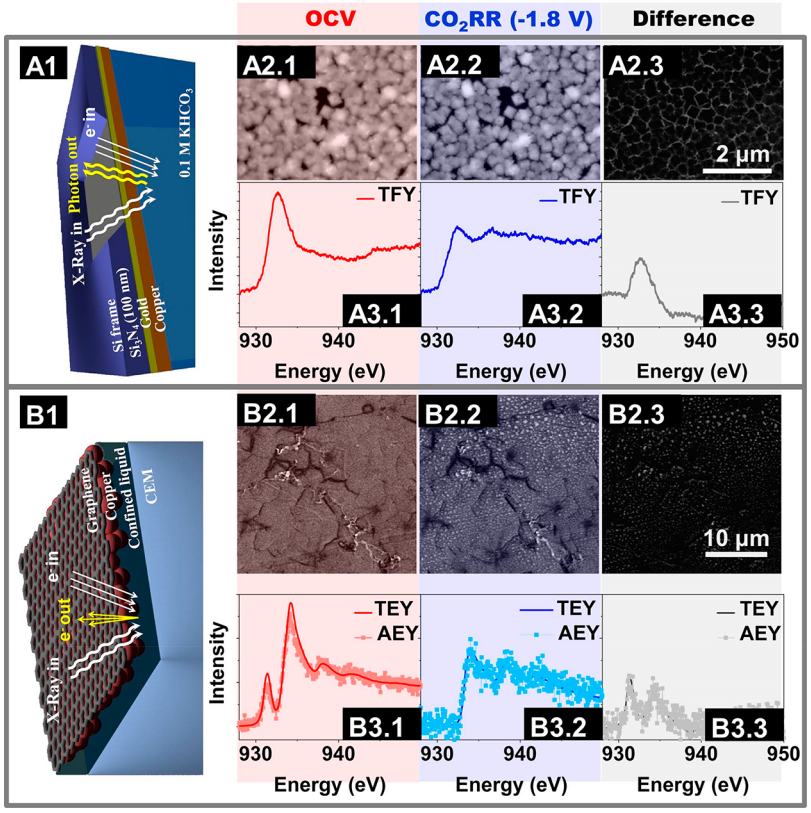

Figure 1. (A1) Schematic drawing of the approach used to investigate electrified electrodes (surface and bulk), which are composed of a photon semitransparent Si_3N_4 membrane (100 nm thick) and electrodeposited Cu electrode onto a 20 nm thick PVD gold electrode. (A2) *In situ* ECSEM measurements in 100 mM $KHCO_3$ saturated in CO_2 under OCV and CO_2RR. (A3) *In situ* XAS measurements in TFY in 100 mM $KHCO_3$ saturated in CO_2 under OCV and −1.8 V vs Ag/AgCl. (B1) Schematic drawing of the approach used to investigate the electrified interface (surface), which is composed of a photoelectron semitransparent single layer of graphene on a CEM. (B2) *In situ* ECSEM measurements in 100 mM $KHCO_3$ saturated in CO_2 under OCV and CO_2RR. (B3) XAS measurements in TEY and AEY in 100 mM $KHCO_3$ under OCV and −1.8 V vs Ag/AgCl.

in transmission mode, yielding information on the whole catalyst.[21] Surface-sensitive contributions under *operando/in situ* conditions are, however, scarce. The reason lies in the short inelastic mean free path (IMFP) of the photoelectrons in dense media.[22] This technical limitation forces the use of *ex situ* characterizations and bulk-sensitive methods, thereby yielding inaccurate pictures of the active/stable copper oxidation state during the CO_2RR. In order to provide an unambiguous description of the oxidation state of copper during the electrocatalytic reduction of CO_2 to valuable hydrocarbons, we enabled the use of surface-sensitive X-ray absorption spectroscopy (XAS) using an atomically thin-film membrane (single-layer graphene) that is semitransparent to the photoelectrons. Furthermore, these results were compared with bulk-sensitive XAS-TFY mode in order to link these changes on the surface with the variations that the catalyst undergoes in the bulk. In addition, we performed *in situ* scanning electron microscopy (SEM) under reaction conditions in the presence of aqueous electrolyte using a continuous flow cell. Previous SEM experiments were limited in the detection of species through a Si_3N_4 window because of a high-contrast effect.[23−27] Furthermore, we overcame the problem of the stability of free-standing graphene reported in the literature during the characterization of liquids[28] for its use in electron spectroscopy and microscopy. Thus, these experiments provide spatial resolution of the modifications that the catalyst undergoes as a consequence of its contact with the liquid electrolyte and applied potential using the same specimen for both microscopy and spectroscopy investigations under *operando* conditions.

First, the change in the electronic structure and morphology of an electrodeposited electrode was investigated during the CO_2RR by means of bulk-sensitive XAS-TFY. In order to do that, we take advantage of an electrochemical cell (EC-cell) based on a thin-film Si_3N_4 membrane (100 nm thick) semitransparent to the incoming X-ray and out-going photons, which enables photon-in/photon-out (PIPO) spectroscopy while still being leak-tight[29,30] (a schematic drawing of this cell operation is shown in Figure 1A1, including the detection scheme). A 20 nm thick Au and 3 nm of Cr (adherence layer) electrode was deposited onto this membrane by physical vapor deposition (PVD) and used as the working electrode for the electrodeposition of copper[31,32] from 50 mM $CuSO_4$ (around ∼300 nm thick as shown in Figure S1A) as described in the Supporting Information. The spectra were collected at the ISISS beamline of the BESSY II synchrotron facility (Berlin, Germany)[33] using a photodiode to collect the TFY signal. In addition, the electrode holder is exchangeable between the *in situ* flow EC-cells compatible with the scanning electron microscopy and TFY spectroscopy setups, allowing the investigation of the same specimen correlating with both techniques. This compatible cell was fabricated and implemented in an environmental scanning electron microscope (ESEM), which we will refer to as electrochemical SEM (ECSEM). It allows for the investigation of electrified electrodes

https://dx.doi.org/10.1021/acsenergylett.0c00802
ACS Energy Lett. 2020, 5, 2106−2111

in the presence of liquid, yielding images with nanometric resolution (more details of this approach can be found in the Supporting Information). Using this setup, copper was electrodeposited on the PVD Au film from a 50 mM $CuSO_4$ solution (see the Supporting Information for more details). Figure 1A2 shows *in situ* ECSEM images of the electrodeposited copper on the Au electrode at OCV in the presence of 100 mM $KHCO_3$ saturated in CO_2. During the CO_2RR (at −1.8 V vs Ag/AgCl) the electrode shrinks, indicating a reduction of the electrode due to oxygen loss from the copper oxide lattice. We measured the relative shrinking on different particles and estimated its distribution (see Figure S2C). On average, the copper phase shrinks by 17% of its original length during reaction, which would correspond to 59% of the original volume for a spherical particle. This result agrees well with the value expected for the reduction of either Cu_2O or CuO into metallic Cu. Furthermore, the reduction of the copper electrode prompts the transformation of a smooth surface into a rough one that contains crevices and channels with more uncoordinated sites which may contribute to the CO_2RR activity/selectivity, as shown in Figure S2. This reduction of the electrode is confirmed by the *in situ* energy-dispersive X-ray spectroscopy (EDX) measurements shown in Figure S3. The EDX spectra indicate a clear decrease in the oxygen signal in line with copper reduction and oxygen loss observed in the *in situ* ECSEM measurements. Unfortunately, EDX is not sensitive enough to the details of the electronic structure, and further investigation with other spectroscopic techniques is required to reveal the atomistic aspects of the electrode under reaction conditions. Using the exchangeable electrode in the *in situ* EC-XAS cell, we investigated the electronic structure of copper during reaction conditions. Figure 1A3 shows the Cu L_3-edges spectra collected in TFY mode depending on the applied potential. Under OCV conditions the electrode is composed of a mixed-oxide of 40% Cu^0 and 60% Cu^+, as determined by fitting the spectrum with a linear combination of reference spectra (Figure S4A). On the other hand, under CO_2RR conditions (−1.8 V vs Ag/AgCl) the electrode is reduced to metallic copper. It is expected that copper oxides are not stable under most of the cathodic potentials at different pH concentrations, as seen in the Pourbaix diagram for copper (see Figure S5),[34] indicating that copper oxide could then only be stabilized because of kinetics during CO_2RR. One should remark at this point that the operation in the *in situ* microreactor cell and in a standard electrochemical setup can be different because of the "current gap" that is related to the difference between the current achievable in both systems being dominated by the cell geometry and charge transport limitations.

TFY-XAS is a bulk-sensitive technique, making it mostly insensitive to the electronic structure modification at the electrified interface. In order to complete the understanding of the CO_2RR process at the electrified interface, we investigated the variation in the electronic structure that an electrodeposited copper electrocatalyst undergoes in the course of the electroreduction of CO_2 to hydrocarbons using Auger electron yield (AEY) and total electron yield (TEY) XAS, which are surface-sensitive techniques because of the short IMFP of the measured electrons (especially AEY-XAS). Thus, we take advantage of an EC-cell based on an ion-conductive membrane[35,36] upgraded to be used with a semitransparent ultrathin working electrode (single-layer graphene), which allows better wetting of the sample (because this membrane acts as a barrier for water evaporation), while retaining an appropriate escape depth of the photoelectrons.[37,38] Distinct from previous work, we replaced the acidic proton exchange membrane (PEM, Nafion) by a cation exchange membrane (CEM, FKD-type sourced from FuMA-Tech GmbH, Bierigheim-Bissingen, Germany) that also allows the transport of OH^-. Figure 1B1 shows the detection scheme and the different parts of this approach, including the electrode, electrolyte, and CEM. Such a sample assembly allows (among other techniques) for X-ray photoelectron spectroscopy at near-ambient pressure (NAPXPS) and ECSEM, even with back scattered electrons. Technical details of the single-layer graphene transfer, EC-cell description and electrodeposited copper electrode preparation can be found in the Supporting Information. After the copper electrode is electrochemically deposited (around ∼300 nm thick as shown in Figure S1B) on the single-layer graphene membrane, 100 mM $HKCO_3$ (saturated in CO_2) electrolyte was flowed into the cell at the same time that the partial pressure of CO_2 in the main chamber was set to 0.5 mbar to ensure it reaches the electrode surface. Using these parameters, we investigated our electrode with *in situ* ECSEM and XAS in TEY and AEY modes. In this manner, Figure 1B2 shows the ECSEM image of the electrodeposited copper in the presence of 100 mM $KHCO_3$ under OCV conditions; after the electrode is polarized to −1.8 V vs Ag/AgCl, there is a modification of the electrode structure, yielding the formation of lumps on the copper surface. Close inspection of the electrode reveals that there is a reconstruction of the electrode as a consequence of the reduction and oxygen loss in the copper lattice. According to these measurements the surface is initially flatter and during the reaction is reconstructed to a rougher surface with more uncoordinated sites, one in good agreement with the previous measurements with the Si_3N_4-based EC-cell. The reconstruction occurs over the whole electrode surface as indicated by the image recorded in a fresh spot (see Figure S6). Furthermore, Figure 1B3 shows the AEY and TEY XAS Cu L_3 edge spectra revealing that the surface is reduced from a mixed copper oxide with a composition of 25% Cu^0, 45% Cu^+, and 30% Cu^{2+} (see Figure S4B) at OCV to metallic copper during CO_2RR. These measurements confirm that the electrified interface is dominated by the formation of reduced copper during the CO_2RR, in good agreement with the TFY-XAS measurements. The modification in the electronic structure of the electrode, surface and bulk, to a more metallic copper, is accompanied by the electrode morphology reconstruction to a rougher one, possibly with remaining dissolved oxygen atoms (known as subsurface oxygen[39,40]) due to slow diffusion/reduction kinetics, during the CO_2RR. The reversibility of the process depending on the applied potential, for both setups, is discussed in the Supporting Information. Therefore, the surface and bulk are in the most stable phase according to the Pourbaix diagram,[34] indicating that it is exactly the same on the surface and in the near-surface of the catalyst where copper oxide can be stabilized only under CO_2RR conditions by the time necessary for the oxygen to diffuse from the bulk to the surface. The experiments reported in this Letter are fully consistent with previous results found recently by Scott et al.[41] using grazing incidence X-ray diffraction (GIXRD) where no copper oxide phase was found during CO_2RR. In addition to the information related to the phase of the copper yielded by the *in situ* GIXRD measurements, the combination of ECSEM/XAS provides an accurate description, with submonolayer sensitivity, of the electronic structure of the catalyst (i.e., oxidation state). X-ray spectroscopy characterization is an element-specific and pure surface-sensitive technique in the case

https://dx.doi.org/10.1021/acsenergylett.0c00802
ACS Energy Lett. 2020, 5, 2106−2111

of the AEY in contrast to GIXRD, which is near-surface-sensitive in the best case. In addition, the *in situ* ECSEM characterization provides important morphology information with nanometric lateral resolution which is not easily accessible with diffraction techniques, indicating that these approaches are complementary. Consequently the results reported in this investigation go a step further in the process description, confirming that the surface of the electrode is reduced to metallic copper with more uncoordinated sites due to surface reconstruction under CO_2RR.

From our experiments it is obvious that the applied potential drives the electrode reduction and oxidation and thus rules the reaction performance. In addition to the previous results, we further investigated the variation in the electronic structure and the products evolved from the reaction depending on the applied cathodic potential. Complete sets of spectra with their respective linear sweep voltammetries (LSV) and reference sample comparison are shown in Figure S7 and S8. These measurements were accomplished in TFY and TEY, the latter being the surface-sensitive measurements more relevant for this investigation. Figure 2A shows how the copper metallicity

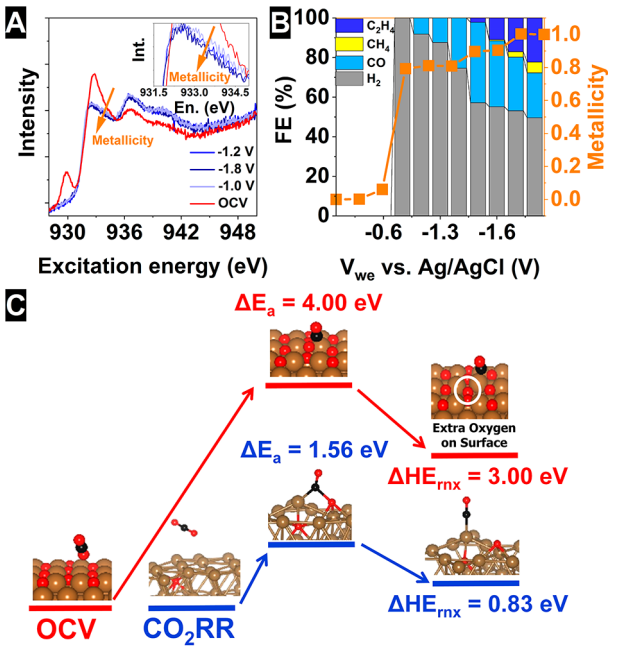

Figure 2. (A) Cu L_3-edge in TEY and (B) Faradaic efficiency for different reaction products depending on the applied potential. (C) Calculations and drawings of the copper structures[32] indicating the difference between Cu_2O under OCV and Cu^0 during the CO_2RR.

increases as the electrode is further reduced at higher cathodic potentials, as indicated by the orange arrow in the figure. In addition, Figure 2B shows the gas-chromatography measurements (GC) of the evolved products depending on the applied potential and the estimated metallicity (in orange). This characterization was done in a setup different than the *in situ* EC-cell (see the Supporting Information for more details). These measurements confirm the unique ability of copper to produce the C−C bond during the electrocatalytic reduction of CO_2, where formic acid is a spectator. The formation of C_2 products is enhanced at more cathodic potentials, indicating that the degree of metallicity, rougher surface, and accumulated charge within the electrical double layer (EDL) controls this process. This result is of the utmost relevance for the CO_2RR. It is obvious from these experiments that the CO_2 reduction is happening on a reduced Cu electrode depending on the applied potential according to the *in situ* spectroscopy. Furthermore, the calculated barrier associated with the dissociative CO_2 adsorption on different copper catalysts[32] indicates that the copper oxide has a higher dissociation barrier due to the formation of extra oxygen on the surface with a CuO-like structure and high dissociation energy, which is the case for OCV conditions, as shown in Figure 2C. Otherwise, when copper is reduced (as during CO_2RR) the dissociation barrier for CO_2 is diminished, facilitating the dissociative adsorption of CO_2 as shown in Figure 2C. Furthermore, based on the ECSEM data, the selective CO_2 reduction toward hydrocarbons probably takes place on a rougher surface controlling the selectivity of the catalysts due to the formation of more uncoordinated sites. Consequently, these experiments indicate that the nature of the reduced copper active sites dominates the activity and selectivity of copper during the reaction. To conclude, one should note that the beam induces water radiolysis, which potentially has several effects on the electrode changes[42] and local redox potential, pH, and temperature.[43] Strategies that were undertaken to mitigate the electron beam interaction with the electrode and electrolyte are discussed in the Supporting Information.

In summary, we first accomplished the investigation of the CO_2RR combining surface and bulk-sensitive *in situ* X-ray absorption spectroscopy with *in situ* ECSEM and GC product analysis using the same specimen. These experiments point out the importance of combining *in situ*/*operando* spectroscopy and microscopy in order to describe accurately the electrode modification during the reactions at certain applied potential. We found direct evidence of the nature of the active sites, which rules the electroreduction of CO_2 to industrially valuable hydrocarbons and alcohols. Under CO_2RR conditions, the surface and the bulk of the electrode are dominated by the existence of reduced copper, which correlates with enhanced C−C bond formation at higher cathodic polarization due to the increased metallicity of the copper electrode. In addition, the formation of reduced copper is accompanied by the electrode reconstruction prompting the formation of a rougher surface that contains crevices and channels with more uncoordinated sites, which in the last term controls the dissociation barrier and thus the activity, selectivity, and stability of the catalysts.

■ ASSOCIATED CONTENT

Supporting Information

The Supporting Information is available free of charge at https://pubs.acs.org/doi/10.1021/acsenergylett.0c00802.

Experimental details (PDF)

Video 1: CA process at −1.8 V vs Ag/AgCl where the bubble formation is due to the CO_2RR and hydrogen evolution reaction (MP4)

Video 2: interaction of the electron beam with the electrode (MP4)

Video 3: interaction of the electron beam with the electrode (MP4)

Video 4: monitoring of corrosion process prompted by the application of anodic polarization (MP4)

Video 5: effect of the electron beam in a pristine membrane coated with graphene (MP4)

Video 6: beam-induced radiolysis process at high magnification in the confined electrolyte in areas with

https://dx.doi.org/10.1021/acsenergylett.0c00802
ACS Energy Lett. 2020, 5, 2106−2111

low electrical conductivity and high hydration as proven by bubble formation (MP4)

AUTHOR INFORMATION

Corresponding Author

Juan-Jesus Velasco-Velez − *Department of Heterogeneous Reactions, Max Planck Institute for Chemical Energy Conversion, Mülheim an der Ruhr 45470, Germany; Department of Inorganic Chemistry, Fritz-Haber-Institut der Max-Planck-Gesellschaft, Berlin 14195, Germany;* orcid.org/0000-0002-6595-0168; Email: velasco@fhi-berlin.mpg.de

Authors

Rik V. Mom − *Department of Inorganic Chemistry, Fritz-Haber-Institut der Max-Planck-Gesellschaft, Berlin 14195, Germany;* orcid.org/0000-0002-5111-5591

Luis-Ernesto Sandoval-Diaz − *Department of Inorganic Chemistry, Fritz-Haber-Institut der Max-Planck-Gesellschaft, Berlin 14195, Germany*

Lorenz J. Falling − *Department of Inorganic Chemistry, Fritz-Haber-Institut der Max-Planck-Gesellschaft, Berlin 14195, Germany;* orcid.org/0000-0002-2622-5166

Cheng-Hao Chuang − *Department of Physics, Tamkang University, New Taipei City 25137, Taiwan*

Dunfeng Gao − *Department of Interface Science, Fritz-Haber-Institute of the Max-Planck Society, 14195 Berlin, Germany; State Key Laboratory of Catalysis, Dalian Institute of Chemical Physics, Chinese Academy of Sciences, 116023 Dalian, China;* orcid.org/0000-0002-2472-7349

Travis E. Jones − *Department of Inorganic Chemistry, Fritz-Haber-Institut der Max-Planck-Gesellschaft, Berlin 14195, Germany;* orcid.org/0000-0001-8921-7641

Qingjun Zhu − *Department of Heterogeneous Reactions, Max Planck Institute for Chemical Energy Conversion, Mülheim an der Ruhr 45470, Germany; Department of Inorganic Chemistry, Fritz-Haber-Institut der Max-Planck-Gesellschaft, Berlin 14195, Germany*

Rosa Arrigo − *School of Science, Engineering and Environment, University of Salford, M5 4 WT Manchester, U.K.;* orcid.org/0000-0002-2877-8733

Beatriz Roldan Cuenya − *Department of Interface Science, Fritz-Haber-Institute of the Max-Planck Society, 14195 Berlin, Germany;* orcid.org/0000-0002-8025-307X

Axel Knop-Gericke − *Department of Heterogeneous Reactions, Max Planck Institute for Chemical Energy Conversion, Mülheim an der Ruhr 45470, Germany; Department of Inorganic Chemistry, Fritz-Haber-Institut der Max-Planck-Gesellschaft, Berlin 14195, Germany*

Thomas Lunkenbein − *Department of Inorganic Chemistry, Fritz-Haber-Institut der Max-Planck-Gesellschaft, Berlin 14195, Germany;* orcid.org/0000-0002-8957-4216

Robert Schlögl − *Department of Heterogeneous Reactions, Max Planck Institute for Chemical Energy Conversion, Mülheim an der Ruhr 45470, Germany; Department of Inorganic Chemistry, Fritz-Haber-Institut der Max-Planck-Gesellschaft, Berlin 14195, Germany*

Complete contact information is available at: https://pubs.acs.org/10.1021/acsenergylett.0c00802

Notes

The authors declare no competing financial interest.

ACKNOWLEDGMENTS

We thank DAAD for financial support in the framework of Taiwanese-German collaboration (Projects ID 57218279 and 57392335). C.-H.C. acknowledges financial support from projects 104-2112-M-032-005-MY2 and 105-2911-I-032-501. D.G. and B.R.C. acknowledge financial support by the German Federal Ministry of Education and Research (Bundesministerium für Bildung und Forschung, BMBF) under Grants #03SF0523C-"CO2EKAT" and #033RCOO4D-"e-Ethylene" and the European Research Council (ERC-725915, OPERANDOCAT). We thank the Helmholtz-Zemtrum Berlin für Materialien und Energie for allocating beamtime for our experiments within the proposal numbers 192-08521 and 191-08014. We thank Eugen Stotz for his support in the design and fabrication of the *in situ* electrochemical cells and Sven Kubala for his help preparing the PVD thin Au electrode onto the Si_3N_4 membranes.

REFERENCES

(1) Schlögl, R. The role of chemistry in the energy challenge. *ChemSusChem* **2010**, *3*, 209−222.

(2) Schlögl, R. The solar refinery. In *Chemical Energy Storage*; De Gruyter, 2013; pp 1−34.

(3) Nitopi, S.; Bertheussen, E.; Scott, S. B.; Liu, X.; Engstfeld, A. K.; Horch, S.; Seger, B.; Stephens, I. E. L.; Chan, K.; Hahn, C.; Nørskov, J. K.; Jaramillo, J. K.; Chorkendorff, I. (2019). Progress and perspectives of electrochemical CO_2 reduction on copper in aqueous electrolyte. *Chem. Rev.* **2019**, *119*, 7610−7672.

(4) Qiao, J.; Liu, Y.; Hong, F.; Zhang, J. A review of catalysts for the electroreduction of carbon dioxide to produce low-carbon fuels. *Chem. Soc. Rev.* **2014**, *43*, 631−675.

(5) Aran-Ais, R. M.; Gao, D.; Roldan Cuenya, B. Structure- and Electrolyte-Sensitivity in CO_2 Electroreduction. *Acc. Chem. Res.* **2018**, *51*, 2906.

(6) Hori, Y.; Kikuchi, K.; Suzuki, S. Production of CO and CH_4 in electrochemical reduction of CO_2 at metal electrodes in aqueous hydrogencarbonate solution. *Chem. Lett.* **1985**, *14*, 1695−1698.

(7) Hori, Y.; Kikuchi, K.; Murata, A.; Suzuki, S. Production of methane and ethylene in electrochemical reduction of carbon dioxide at copper electrode in aqueous hydrogencarbonate solution. *Chem. Lett.* **1986**, *15*, 897−898.

(8) Hori, Y.; Murata, A.; Takahashi, R. Formation of hydrocarbons in the electrochemical reduction of carbon dioxide at a copper electrode in aqueous solution. *J. Chem. Soc., Faraday Trans. 1* **1989**, *85*, 2309−2326.

(9) Hori, Y.; Takahashi, I.; Koga, O.; Hoshi, N. Selective formation of C_2 compounds from electrochemical reduction of CO_2 at a series of copper single crystal electrodes. *J. Phys. Chem. B* **2002**, *106*, 15−17.

(10) Li, C. W.; Kanan, M. W. CO_2 reduction at low overpotential on Cu electrodes resulting from the reduction of thick Cu_2O films. *J. Am. Chem. Soc.* **2012**, *134*, 7231−7234.

(11) Kas, R.; Kortlever, R.; Milbrat, A.; Koper, M. T. M.; Mul, G.; Baltrusaitis, J. Electrochemical CO_2 reduction on Cu_2O-derived copper nanoparticles: controlling the catalytic selectivity of hydrocarbons. *Phys. Chem. Chem. Phys.* **2014**, *16*, 12194−12201.

(12) Jermann, B.; Augustynski, J. Long-term activation of the copper cathode in the course of CO_2 reduction. *Electrochim. Acta* **1994**, *39*, 1891−1896.

(13) Gao, D.; Aran-Ais, R. M.; Jeon, H. S.; Roldan Cuenya, B. Rational catalyst and electrolyte design for CO_2 electroreduction towards multicarbon products. *Nat. Catal.* **2019**, *2* (3), 198−210.

(14) Handoko, A. D.; et al. Mechanistic Insights into the Selective Electroreduction of Carbon Dioxide to Ethylene on Cu_2O-Derived Copper Catalysts. *J. Phys. Chem. C* **2016**, *120* (36), 20058−20067.

(15) Velasco-Velez, J. J.; Wu, C. H.; Pascal, T. A.; Wan, L. F.; Guo, J.; Prendergast, D.; Salmeron, M. The structure of interfacial water on gold electrodes studied by x-ray absorption spectroscopy. *Science* **2014**, *346*, 831.

(16) Itkis, D. M.; Velasco-Velez, J. J.; Knop-Gericke, A.; Vyalikh, A.; Avdeev, M.; Yashina, L. V. Probing operating electrochemical interfaces by photons and neutrons. *ChemElectroChem* **2015**, *2*, 1427−1445.
(17) Mistry, H.; Varela, A. S.; Bonifacio, C. S.; Zegkinoglou, I.; Sinev, I.; Choi, Y.-W.; Kisslinger, K.; Stach, E. A.; Yang, J. C.; Strasser, P.; Roldan Cuenya, B. Highly selective plasma-activated copper catalysts for carbon dioxide reduction to ethylene. *Nat. Commun.* **2016**, *7*, 12123.
(18) Gao, D.; Zegkinoglou, I.; Divins, N. J.; Scholten, F.; Sinev, I.; Grosse, P.; Roldan-Cuenya, B. Plasma-Activated Copper Nanocube Catalysts for Efficient Carbon Dioxide Electroreduction to Hydrocarbons and Alcohols. *ACS Nano* **2017**, *11*, 4825.
(19) Jiang, P.; Chen, J. L.; Borondics, F.; Glans, P. A.; West, M. W.; Chang, C. L.; Salmeron, M.; Guo, J. In situ soft X-ray absorption spectroscopy investigation of electrochemical corrosion of copper in aqueous $NaHCO_3$ solution. *Electrochem. Commun.* **2010**, *12*, 820−822.
(20) Velasco-Vélez, J. J.; Jones, T. E.; Pfeifer, V.; Dong, C. L.; Chen, Y. X.; Chen, C. M.; Lu, Y. R.; Chen, J. M.; Schlögl, R.; Knop-Gericke, A.; Chuang, C. H. Trends in reactivity of electrodeposited 3d transition metals on gold revealed by operando soft x-ray absorption spectroscopy during water splitting. *J. Phys. D: Appl. Phys.* **2017**, *50*, 024002.
(21) Schwanke, C.; Xi, L.; Lange, K. M. A soft XAS transmission cell for operando studies. *J. Synchrotron Radiat.* **2016**, *23*, 1390−1394.
(22) Velasco-Velez, J. J.; Pfeifer, V.; Hävecker, M.; Weatherup, R.; Arrigo, R.; Chuang, C. H.; Stotz, E.; Weinberg, G.; Salmeron, M.; Schlögl, R.; Knop-Gericke, A. Photoelectron spectroscopy at the graphene−liquid interface reveals the electronic structure of an electrodeposited cobalt/graphene electrocatalyst. *Angew. Chem., Int. Ed.* **2015**, *54*, 14554−14558.
(23) Suga, M.; Nishiyama, H.; Konyuba, Y.; Iwamatsu, S.; Watanabe, Y.; Yoshiura, C.; Ueda, T.; Sato, C. The atmospheric scanning electron microscope with open sample space observes dynamic phenomena in liquid or gas. *Ultramicroscopy* **2011**, *111*, 1650−1658.
(24) Ominami, Y.; Kawanishi, S.; Ushiki, T.; Ito, S. A novel approach to scanning electron microscopy at ambient atmospheric pressure. *Microscopy* **2015**, *64*, 97−104.
(25) Han, Y.; Nguyen, K. X.; Ogawa, Y.; Park, J.; Muller, D. A. Atomically thin graphene windows that enable high contrast electron microscopy without a specimen vacuum chamber. *Nano Lett.* **2016**, *16*, 7427−7432.
(26) Rong, G.; Zhang, X.; Zhao, W.; Qiu, Y.; Liu, M.; Ye, F.; Xu, Y.; Hou, Y.; Li, W.; Duan, W.; Zhang, Y. Liquid-Phase Electrochemical Scanning Electron Microscopy for In Situ Investigation of Lithium Dendrite Growth and Dissolution. *Adv. Mater.* **2017**, *29*, 1606187.
(27) Kang, I. H.; Kim, D. M.; Kim, Y. M. Liquid Phase Electron Microscopy Study on the Growth Mechanism of Gold Nanoparticles: In Scanning Electron Microscope. *Microsc. Microanal.* **2019**, *25*, 1504−1505.
(28) Knop-Gericke, A.; Pfeifer, V.; Velasco-Velez, J. J.; Jones, T.; Arrigo, R.; Hävecker, M.; Schlögl, R. In situ X-ray photoelectron spectroscopy of electrochemically active solid-gas and solid-liquid interfaces. *J. Electron Spectrosc. Relat. Phenom.* **2017**, *221*, 10−17.
(29) Velasco-Velez, J. J.; Chuang, C. H.; Han, H. L.; Martin-Fernandez, I.; Martinez, C.; Pong, W. F.; Shen, Y. R.; Wang, F.; Zhang, Y.; Guo, J.; Salmeron, M. In-situ XAS investigation of the effect of electrochemical reactions on the structure of graphene in aqueous electrolytes. *J. Electrochem. Soc.* **2013**, *160*, C445−C450.
(30) Velasco-Velez, J. J.; Wu, C. H.; Wang, B. Y.; Sun, Y.; Zhang, Y.; Guo, J.-H.; Salmeron, M. Polarized X-ray absorption spectroscopy observation of electronic and structural changes of chemical vapor deposition graphene in contact with water. *J. Phys. Chem. C* **2014**, *118*, 25456−25459.
(31) Velasco-Vélez, J. J.; Skorupska, K.; Frei, E.; Huang, Y. C.; Dong, C. L.; Su, B. J.; Hsu, C. C.; Chou, H. Y.; Chen, J. M.; Strasser; Schlögl, R.; Knop-Gericke, A.; Chuang, C. H. The Electro-Deposition/Dissolution of $CuSO_4$ Aqueous Electrolyte Investigated by In Situ Soft X-ray Absorption Spectroscopy. *J. Phys. Chem. B* **2018**, *122*, 780−787.
(32) Velasco-Vélez, J. J.; Jones, T.; Gao, D.; Carbonio, E.; Arrigo, R.; Hsu, C.-J.; Huang, Y. C.; Dong, C. L.; Chen, J. M.; Lee, J. F.; Strasser, P.; Roldan-Cuenya, B.; Schlögl, R.; Knop-Gericke, A.; Chuang, C. H. The role of the copper oxidation state in the electrocatalytic reduction of CO_2 into valuable hydrocarbons. *ACS Sustainable Chem. Eng.* **2019**, *7*, 1485−1492.
(33) Vass, E. M.; Hävecker, M.; Zafeiratos, S.; Teschner, D.; Knop-Gericke, A.; Schlögl, R. The role of carbon species in heterogeneous catalytic processes: an in situ soft x-ray photoelectron spectroscopy study. *J. Phys.: Condens. Matter* **2008**, *20* (18), 184016.
(34) Pourbaix, M. *Atlas of electrochemical equilibria in aqueous solutions*, 2nd English ed.; National Association of Corrosion Engineers: Houston, TX, 1974.
(35) Arrigo, R.; Hävecker, M.; Schuster, M. E.; Ranjan, C.; Stotz, E.; Knop-Gericke, A.; Schlögl, R. In Situ Study of the Gas-Phase Electrolysis of Water on Platinum by NAP-XPS. *Angew. Chem., Int. Ed.* **2013**, *52* (44), 11660−11664.
(36) Streibel, V.; Hävecker, M.; Yi, Y.; Vélez-Velasco, J. J.; Skorupska, K.; Stotz, E.; Knop-Gericke, A.; Schlögl, R.; Arrigo, R. In situ electrochemical cells to study the oxygen evolution reaction by near ambient pressure X-ray photoelectron spectroscopy. *Top. Catal.* **2018**, *61* (20), 2064−2084.
(37) Frevel, L. J.; Mom, R.; Velasco-Vélez, J. J.; Plodinec, M.; Knop-Gericke, A.; Schlögl, R.; Jones, T. E. In Situ X-ray Spectroscopy of the Electrochemical Development of Iridium Nanoparticles in Confined Electrolyte. *J. Phys. Chem. C* **2019**, *123*, 9146−9152.
(38) Mom, R.; Frevel, L.; Velasco-Vélez, J. J.; Plodinec, M.; Knop-Gericke, A.; Schlögl, R. The Oxidation of Platinum under Wet Conditions Observed by Electrochemical X-ray Photoelectron Spectroscopy. *J. Am. Chem. Soc.* **2019**, *141*, 6537−6544.
(39) Eilert, A.; Cavalca, F.; Roberts, F. S.; Osterwalder, J.; Liu, C.; Favaro, M.; Crumlin, E.; Ogasawara, H.; Friebel, D.; Pettersson, L. G. M.; Nilsson, A. Subsurface oxygen in oxide-derived copper electrocatalysts for carbon dioxide reduction. *J. Phys. Chem. Lett.* **2017**, *8*, 285−290.
(40) Knop-Gericke, A.; Hävecker, M.; Schedel-Niedrig, T.; Schlögl, R. Probing the electronic structure of an active catalyst surface under high-pressure reaction conditions: the oxidation of methanol over copper. *Catal. Lett.* **2000**, *66*, 215−220.
(41) Scott, S. B.; Hogg, T. V.; Landers, A. T.; Maagaard, T.; Bertheussen, E.; Lin, J. C.; Davis, R. C.; Beeman, J. W.; Higgins, D.; Drisdell, W.; Hahn, C.; Mehta, A.; Seger, B.; Jaramillo, T. F.; Chorkendorff, I. (2019). Absence of oxidized phases in Cu under CO reduction conditions. *ACS Ener. Lett.* **2019**, *4* (3), 803−804.
(42) Schneider, N. M.; Norton, M. M.; Mendel, B. J.; Grogan, J. M.; Ross, F. M.; Bau, H. H. Electron−water interactions and implications for liquid cell electron microscopy. *J. Phys. Chem. C* **2014**, *118* (38), 22373−22382.
(43) Ambrožič, B.; Prašnikar, A.; Hodnik, N.; Kostevšek, N.; Likozar, B.; Rožman, K. Ž.; Šturm, S. Controlling the radical-induced redox chemistry inside a liquid-cell TEM. *Chem. Sci.* **2019**, *10* (38), 8735−8743.

https://dx.doi.org/10.1021/acsenergylett.0c00802
ACS Energy Lett. 2020, 5, 2106−2111